Surgery-induced neuroinflammatory transcriptional programs in medial prefrontal cortex of mice during early phase of perioperative neurocognitive disorders

Xiaodong Tang*, Xuwu Xiang*, Yang Yu, Shuyuan Huang, Caifei Pan, Shuyuan Gan and Yongxing Yao

Department of Anesthesiology, First Affiliated Hospital, Zhejiang University School of Medicine, Hangzhou, Zhejiang, China

* These authors contributed equally to this work.

ABSTRACT

Patients receiving anesthesia and surgery may experience cognitive dysfunction, memory deficits, and mental disturbances, which are referred to as perioperative neurocognitive disorders (PND). The function of the medial prefrontal cortex (mPFC) is disrupted during early phase of PND. To gain insight into the mechanisms of PND, we collected mouse mPFC tissues 6 h post-surgery and performed RNA sequencing analysis. In total, 178 differentially expressed genes (DEGs) were identified, including 105 upregulated and 73 downregulated genes. Bioinformatic analysis highlighted the significant enrichment of these DEGs in several immune-related biological processes and signaling pathways, suggesting that pronounced neuroinflammatory transcriptional programming in the mPFC was evoked during early phase of PND. Interleukin-6 level increased in both serum and mPFC, while the mRNA levels of *Il-6*, *Tnf*-α, and *Il-1β* remained unchanged. Taken together, our findings suggest that a distinct and acute neuroinflammatory response in the mPFC is evoked after peripheral surgery, which might play a key role in the development of PND.

Subjects Genomics, Molecular Biology, Neuroscience, Cognitive Disorders, Surgery and Surgical Specialties

Keywords Surgery, Cognitive dysfunction, RNA sequencing, Neuroinflammation, Medial prefrontal cortex

INTRODUCTION

After anesthesia and surgery, some patients experience issues in concentrating, learning and memory impairments, and executive dysfunction, which can last for weeks or months (*Moller et al., 1998*; *Evered et al., 2018*). Perioperative neurocognitive disorders (PND) occur in 4.7–23.8% patients undergone surgery (*Berian et al., 2018*; *Silva et al., 2021*), leading to various adverse outcomes including prolonged hospitalization, increased morbidity and mortality, decreased quality of life, and an increased long-term risk of

Submitted 20 September 2024
Accepted 18 November 2024
Published 3 December 2024

Corresponding author
Yongxing Yao,
yaoyongxing@zju.edu.cn

Academic editor
Tiziano Balzano

Additional Information and Declarations can be found on page 13

DOI **10.7717/peerj.18664**

How to cite this article Tang X, Xiang X, Yu Y, Huang S, Pan C, Gan S, Yao Y. 2024. Surgery-induced neuroinflammatory transcriptional programs in medial prefrontal cortex of mice during early phase of perioperative neurocognitive disorders. **PeerJ 12:e18664**
DOI 10.7717/peerj.18664

Alzheimer's disease (*Robinson et al., 2009*). However, the underlying mechanisms of PND remain poorly understood.

Associative fear learning constitutes a defensive motivational system evolved to safeguard against environmental threats, involving stages such as acquisition/encoding, consolidation, retrieval, and extinction (*Johansen et al., 2011*). In PND models, mice exhibit a diminished response to associative threats following surgery, and fear conditioning is a widely used behavioral paradigm (*Sun et al., 2023*; *Ma et al., 2024*). Neuronal activity in the medial prefrontal cortex (mPFC) is essential for fear memory (*Courtin et al., 2013*; *Agetsuma et al., 2023*). Synaptic transmission is impaired in a subregion of the mPFC after surgery (*Sun et al., 2023*). Furthermore, the functional connectivity within the dorsal hippocampus-mPFC circuit is disrupted after surgery (*Chen et al., 2022*; *Ma et al., 2024*). The activities of mPFC-amygdala projections are dysregulated acutely after surgery (*Sun et al., 2023*). However, the molecular mechanisms underlying early degeneration of the mPFC remain unclear.

Considering the implications of mRNAs dysregulation in neurological disorders, investigating its role in PND pathogenesis is crucial. However, peripheral surgery-induced transcriptional responses in the mPFC during early phase remain unknown. In this study, we identified distinct immune response-related features in the mPFC of mice during early phase of PND by analyzing global transcriptomic changes and evaluating the levels of several proinflammatory cytokines.

MATERIALS AND METHODS

Animals and experimental design

A total of 61 male C57BL/6J mice (10–14 week-old; 25–30 g) were purchased from Shanghai SLAC Laboratory Animal Co. Ltd. (Shanghai, China) and acclimated for 2 weeks. All mice were housed in ventilated cages (485 × 200 × 200 mm; 4–5 mice per cage) in standard conditions (12-h light/12-h dark cycle, lights on at 8 am; temperature, 22–24 °C; humidity, 55 ± 10%) with *ad libitum* access to water and food. Mice were tagged and randomly allocated to each group before any procedure. For open-field test, 10 mice were used in control and surgery groups; for fear conditioning test, 11 mice were used in control and surgery groups; for RNA sequencing (RNA-seq) and quantitative real-time polymerase chain reaction (qRT–PCR), three mice were used in control and surgery groups; for enzyme-linked immunosorbent assay (ELISA), 6–7 mice were used in control and surgery groups. Since whole blood and mPFC tissue collection were required for this study, mice were euthanized at the conclusion of the experimental period. Euthanasia was performed using 1% pentobarbital sodium (50 mg/kg, intraperitoneal injection). All animal experiments were approved by the Animal Care Committee of the First Affiliated Hospital at Zhejiang University School of Medicine (approval number: 2022-1435) and were conducted in compliance with the Animal Research Reporting *In Vivo* Experiments (ARRIVE) guidelines and the National Institutes of Health Guide for the Care and Use of Laboratory Animals.

Surgery of tibial fracture

We used a clinically relevant mouse model of tibial fracture. The postoperative changes in these mice mimic certain cognitive impairments commonly observed in humans after routine orthopedic surgery, while exhibiting no apparent impact on sensory function and motor activities during behavioral tests (*Xiong et al., 2018*; *Xiang et al., 2022*). Mice underwent aseptic open tibial fracture surgery with intramedullary fixation under general anesthesia, as previously described (*Xiang et al., 2022*). Briefly, general anesthesia consisted of induction with 3.0% isoflurane followed by maintenance with 2.0% isoflurane in 30% FiO_2. To expose the tibia, a median incision was made on the disinfected left paw. A 0.38-mm needle was inserted into the tibial medullary cavity, followed by osteotomy of the tibia at the junction of the middle and distal thirds. The fixation needle was left in place, trimmed flush with the tibial cortex, and the skin was sutured. The entire procedure from induction of anesthesia to the end of surgery was completed within 15 min. Mice were allowed to recover spontaneously from anesthesia. Throughout the surgery and recovery, body temperature was maintained at 37 °C using a heating pad. Analgesia (30 mg/kg tramadol) was subcutaneously administered after induction of anesthesia and prior to skin incision. Mice in the control group received identical anesthesia and analgesia but underwent no surgical procedures.

Open-field test

An open-field test was conducted to evaluate the spontaneous locomotor activity and anxiety levels in mice 24 h post-surgery. The apparatus consisted of a 50 cm × 50 cm open arena with 50 cm high walls and a floor divided into 25 equal squares. Briefly, mice were placed individually in the center of the apparatus and allowed to habituate and explore freely for 10 min. The total distance traveled and time spent in the center were automatically recorded using ANY-maze behavior tracking software (Stoelting Co., Wood Dale, IL, USA). The arena was thoroughly cleaned with 75% ethanol between trials.

Fear conditioning test

The contextual and cued fear conditioning test is a behavioral paradigm used to assess learning and memory. Freezing behavior, defined as complete immobility except for breathing, is a typical natural response to fearful situations. The extent of fear learning was recorded in a fear-conditioning chamber (Shanghai Xinruan Information Technology Co. Ltd., Shanghai, China). A decrease in freezing time indicated memory impairment.

Training

Mice were habituated to handling for 3 days before the behavioral tests. On the training day, mice were individually placed in the conditioning chamber and allowed to explore freely for 2 min. Subsequently, an auditory cue (80 dB, 400 Hz, conditional stimulus) was presented for 30 s and co-terminated with a 2-s foot shock (0.5 mA, unconditional stimulus). Three tone-foot shock parings were delivered at an inter-trial interval of 15 s. Mice were kept in the training chamber for another 2 min before being returned to their home cages.

Testing

Three days after the training session, mice were returned to the original conditioning chamber for 4 min without any tone or foot shock. Freezing behavior during this session was scored to assess contextual fear memory. After 6 h, mice were placed in another chamber with altered stripes and background odor, and were allowed to explore for 2 min. Mice were then exposed to an auditory stimulus (80 dB, 400 Hz) for 2 min, and the freezing duration was recorded to evaluate cued fear memory. The time spent freezing as a fraction of the total time spent in the chamber was recorded using a video-tracking system.

RNA-seq analysis

Total RNA was extracted from the mPFC of mice of the Control and Surgery groups (three mice in each group) using TRIzol Reagent (Invitrogen, Carlsbad, CA, USA), and digested with RNase-Free DNase to remove residual DNAs. RNA quality was assayed on an Nanodrop ND-1000 spectrophotometer (Thermo Fisher Scientific, Waltham, MA, USA), and all samples sequenced exhibited an RIN > 8.0. Then, the poly (A) mRNA was enriched by oligo (dT)-attached magnetic beads and followed by fragmented into small pieces using fragmentation reagent. The RNA fragments were copied into first-strand cDNA using reverse transcriptase and random primers. Then second-strand cDNA was synthesized using the prepared second-strand synthesis reaction system. These cDNA fragments then had the addition of a single "A" base and subsequent ligation of the adapter. Library construction and sequencing were performed using a BGISEQ500 platform (BGI-Shenzhen, China). All raw data were deposited in the National Center for Biotechnology Information Sequence Read Archive database (accession ID: PRJNA1077729). The sequencing data were filtered using SOAPnuke (v1.5.2), and clean reads were mapped to the mouse reference genome (mm10) using HISAT2 (v2.0.4). Gene quantification was performed using RSEM (v1.3.1), and expression was quantified as fragments per kilobase of transcript per million mapped reads (FPKM). DESeq2 (v1.4.5) was used to identify differentially expressed genes (DEGs) between the groups. The adjusted *p*-value, termed Q value, was calculated by controlling false discovery rate. Fold changes (FC) of DEGs were determined based on the FPKM values. DEGs were identified using the criteria of $|\log_2 FC| \geq 1$ and Q value ≤ 0.05. To gain insight into phenotypic changes, Gene Ontology (GO, http://www.geneontology.org/) and Kyoto Encyclopedia of Genes and Genomes (KEGG, https://www.kegg.jp/) enrichment analyses of the annotated DEGs were performed. GO and KEGG terms were ranked by Q value, and a Q value ≤ 0.05 served as the cutoff criterion. The statistical power of this experimental design, calculated in RNASeqPower (An online implementation of RNASeqPower is available at https://rodrigo-arcoverde.shinyapps.io/rnaseq_power_calc/) is 0.83. There are six biological and technical replicates used to achieve the claimed statistical power.

qRT–PCR

RNA was reverse-transcribed into cDNA using the PrimeScriptTMRT Reagent Kit (Takara, Shiga, Japan), in accordance with the manufacturer's instructions. qRT–PCR was performed using a QuantStudio5 thermocycler (Thermo Fisher Scientific, Waltham, MA,

USA) and the SYBR Premix EX TaqTM II kit (Takara, Shiga, Japan) following the manufacturer's instructions. Amplification was performed starting with an initial denaturation step at 95 °C for 30 s, followed by 40 cycles of 95 °C for 5 s and 60 °C for 31 s, in 10 μL reaction volume. All samples were amplified in triplicate, and the mean value was used for subsequent calculations. The fold changes in mRNA expression were calculated using the $2^{-\Delta\Delta Ct}$ method, and glyceraldehyde-3-phosphate dehydrogenase (GAPDH) was used as an internal control. The sequences of primer pairs for the target genes are listed in Table S1. All PCR experiments and analyses adhered to the MIQE guidelines.

Measurement of cytokine levels

After mice were deeply anesthetized, whole blood was collected *via* left ventricular puncture. The blood samples were centrifuged at 3,000×*g* for 15 min at 4 °C, and serum was separated and immediately stored at −80 °C until analysis. Subsequently, mice were transcardially perfused with ice cold saline, and the mPFC tissues were dissected on ice under microscopic observation as previously described (*Xu et al., 2016*), immediately frozen in liquid nitrogen, and stored at −80 °C for further processing. Specifically, 1-mm-thick coronal brain sections were prepared by using a mouse brain mold. The mPFC tissue was then identified and collected with a biopsy punch based on the mouse brain atlas (*Paxinos & Franklin, 2019*), targeting the region approximately 2.3–1.3 mm anterior to the bregma, encompassing the cingulate, prelimbic and infralimbic subregions. The mPFC tissues were homogenized in NP-40 lysis buffer containing protease and phosphatase inhibitors (Beyotime Biotech, Shanghai, China), and were centrifuged at 12,000×*g* for 10 min at 4 °C. The supernatant was collected for analysis. Total protein content in the supernatant was quantified using a BCA protein assay kit (Thermo Fisher Scientific, Waltham, MA, USA). A commercially available ELISA kit for detecting Interleukin (IL)-6 level in mice (R&D Systems, Minneapolis, MN, USA) was used according to the manufacturer's instructions.

Statistical analysis

Statistical analyses were performed using GraphPad Prism software (v7.0; Prism Software Inc., San Diego, CA, USA). Data are expressed as mean ± standard error of the mean (SEM). Comparisons between two groups were performed using an unpaired two-tailed student's *t*-test, assuming equal variance. No data points were excluded from the statistical analysis. $P < 0.05$ was considered statistically significant.

RESULTS

Cognitive decline after surgery

An aseptic model of tibial fracture surgery was established to investigate the underlying mechanisms of PND. Cognitive performance was assessed using a fear conditioning paradigm (Fig. 1A). Compared to that of the anesthesia-matched control group, the surgery group exhibited a significant decrease in freezing time in contextual and cued fear memory tests (Figs. 1B and 1C), suggesting that fear memory performance was impaired after surgery. In a separate cohort, in the open-field test (Figs. 1D and 1E), there was no

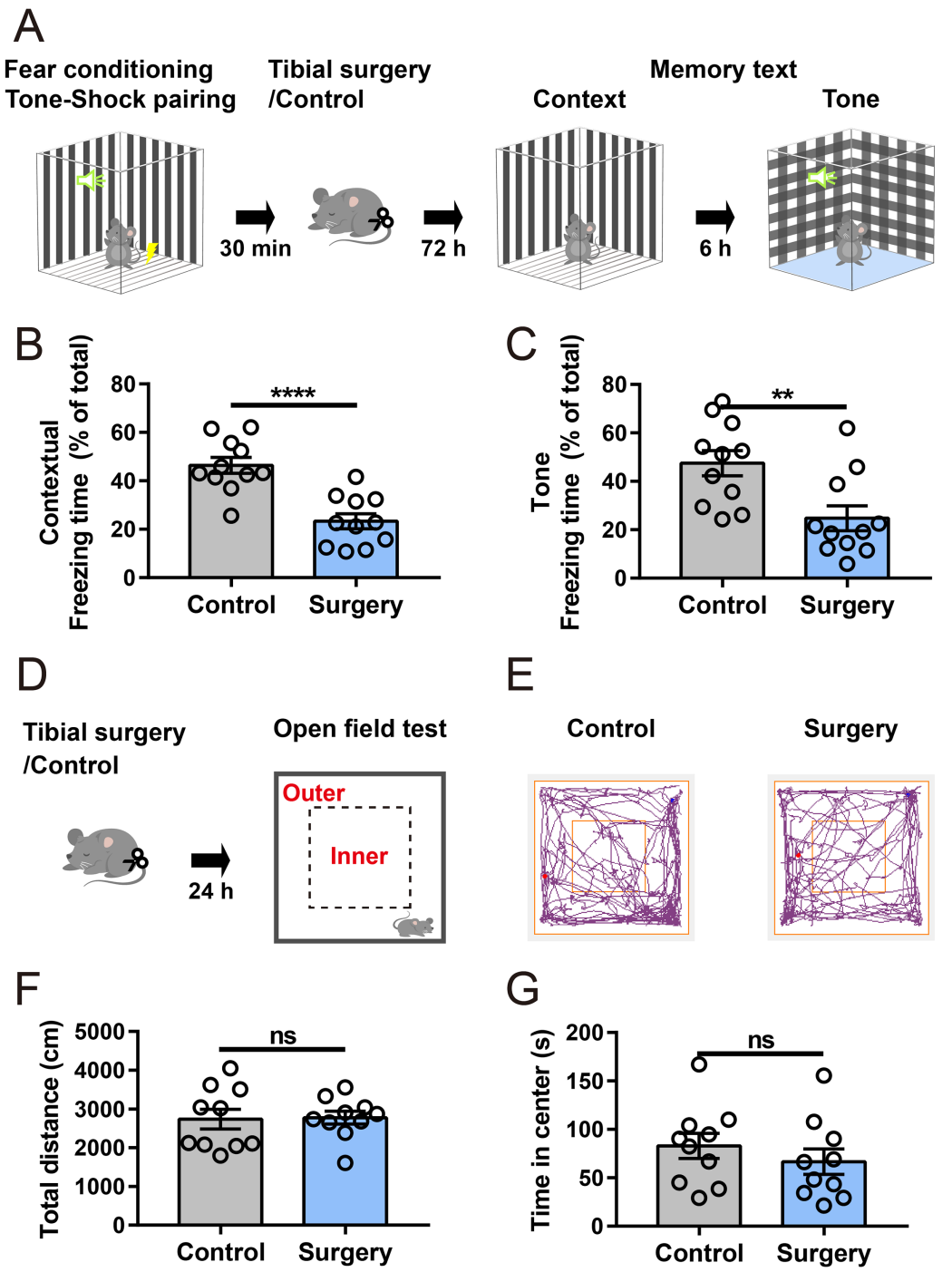

Figure 1 Tibial surgery leads to cognitive decline. (A) Experiment paradigm, cartoon depicting the paradigm of contextual and cued fear conditioning behaviors. (B and C) Percent of time spent in freezing behavior (n = 11 mice/group). (D) Experimental paradigm, cartoon depicting the open field test. The open field is divided into 5 × 5 square bins, with 16 outer bins defined as the outer zone and the remaining area as the inner zone. (E) Representative tracings of the open field activity in control and surgery mice. (F) Total distance traveled in the open field and (G) Time spent in the center of the open field during test (n = 10 mice/group). Data are represented as mean ± SEM, ****P < 0.0001; **P < 0.01; ns, not significant. Full-size DOI: 10.7717/peerj.18664/fig-1

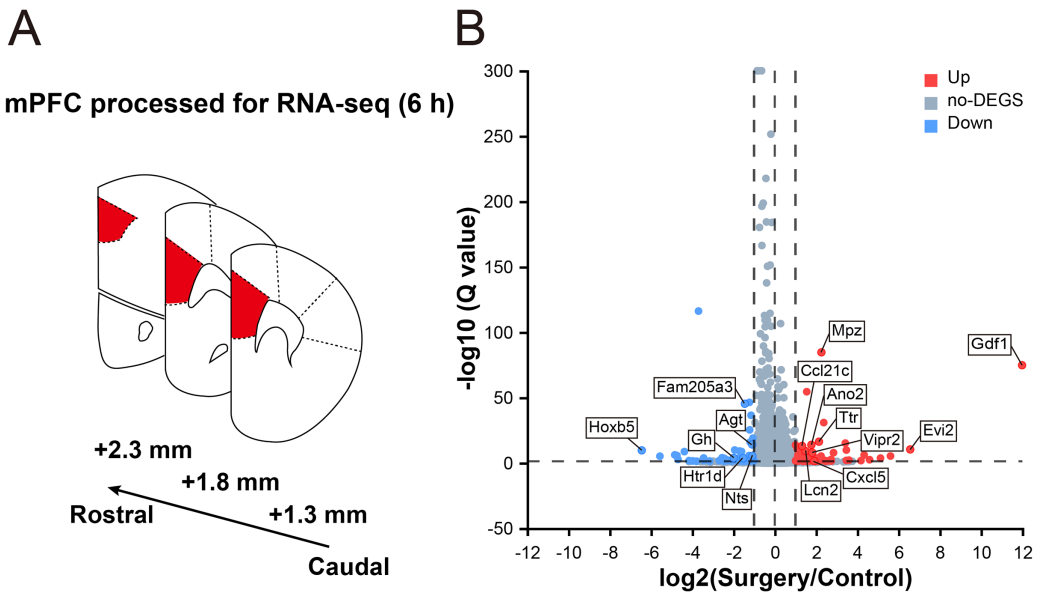

Figure 2 Transcriptomic changes in the mPFC in mice at 6 h after surgery. (A) Schematic coronal section of rat brain illustrating the mPFC according the rat brain atlas (approximately 2.3–1.3 mm anterior from the bregma). (B) Volcano plot illustrating DEGs between the surgery and control groups. Several main DEGs are annotated. Upregulated genes are labeled in red, downregulated in blue, and the rest in gray. $|\log_2 FC| \geq 1$, Q value ≤ 0.05 used as screening threshold, $n = 3$ mice/group.
Full-size DOI: 10.7717/peerj.18664/fig-2

significant difference in the total distance traveled between the control and surgery group (Fig. 1F), indicating spontaneous locomotor activity was not impaired after surgery. Additionally, time spent in the center zone of the open field was comparable between the two groups (Fig. 1G), suggesting no substantial difference in anxiety-like behaviors.

Transcriptome profile in the mPFC

To reveal the surgery-induced changes in the mPFC at the transcriptional level, RNA-seq analysis and DEG screening were performed on six samples collected 6 h after surgery (three mice in each group, Fig. 2A). The sequencing generated, on an average, 66.90 million clean reads with a clean read ratio of 93.02%. From the mouse reference genome, 18,029 mRNAs were identified, corresponding to 202,923 genes.

In total, 178 genes were differentially expressed between control and surgery mice (Table S2), and 105 were upregulated ($\log_2 FC \geq 1$, Q value ≤ 0.05), while 73 were downregulated ($\log_2 FC \leq -1$, Q value ≤ 0.05) (Fig. 2B). These findings indicated that significant reprogramming of gene expression in the mPFC was acutely induced after surgery.

GO enrichment analysis

To gain insight into the functions of these DEGs, GO analysis was performed, and the DEGs were categorized into three distinct ontologies such as biological process (BP), cellular component (CC), and molecular function (MF).

In the BP category (Fig. 3A), among the 20 top enriched terms, the majority were related with immune processes, including leukocyte chemotaxis, lymphocyte chemotaxis, monocyte chemotaxis, chemokine-mediated signaling pathway, neutrophil chemotaxis, cellular response to IL-1, positive regulation of neutrophil differentiation, cellular response to tumor necrosis factor (TNF), response to bacterium, positive regulation of mononuclear cell migration, astrocyte activation, inflammatory response and cellular response to interferon-gamma (IFN-γ), which suggest a significant involvement of immune activity. In the CC category (Fig. 3B), the enriched terms included NADPH oxidase complex, protein complex involved in cell adhesion, T cell receptor complex and immunological synapse. Regarding the MF class (Fig. 3C), several enriched GO terms pertained to inflammation-related binding processes, including chemokine activity, CCR7 chemokine receptor binding, CCR chemokine receptor binding, chemokine receptor binding, cytokine activity and IL-6 receptor binding. These findings suggest an active inflammatory response in the mPFC region.

KEGG pathway analysis

To further elucidate the biological functions of the identified DEGs, KEGG pathway enrichment analysis was performed. Surprisingly, the three top significantly enriched pathway terms were cytokine–cytokine receptor interaction, nuclear factor kappa beta signaling pathway, and chemokine signaling pathway (Fig. 3D). Moreover, several pathways associated with neurogenic diseases (neuroactive ligand–receptor interaction, cell adhesion molecules, and tight junction) were among the 20 top enriched terms. Of note, several inflammation-related pathways involved in signal transduction were also enriched, including cAMP, Jak-STAT, TNF and IL-17 signaling pathways, Th1 and Th2 cell differentiation, complement and coagulation cascades, and Toll-like receptor signaling pathway. Together with GO analysis, these results suggest the presence of neuroinflammation and significant neuroinflammatory transcriptional reprogramming in the mPFC during the early phase of PND.

qRT–PCR validation of RNA-seq results

To validate the RNA-seq data, 15 DEGs of interest were selected for qRT–PCR analysis. The DEGs were both statistically robust and biologically relevant to neuroinflammatory pathways or cognitive function, aligning with our study's focus (Table S3). Their expression analyzed by qRT–PCR exhibited changes similar to the RNA-seq data (Figs. 4B and 4C), with 10 genes (*Vipr2*, *Lcn2*, *Cxcl5*, *Ccl21c*,*Ttr*, *Cybb*, *Ano2*, *Scgn*, *Lrg1*, and *Cd28*) upregulated and five (*Nts*, *Gh*, *Stat4*, *Htr1d*, and *Agt*) downregulated. Among them, *Vipr2*, *Lcn2*, *Ttr*, *Ano2*, *Scgn*, *Gh*, *Nts*, and *Agt* have been implicated in neurological dysfunction and disease, and *Lcn2*, *Cxcl5*, *Ccl21c*, *Cybb*, and *Cd28* play roles in immune responses. Other genes selected for qRT–PCR analysis included *Lrg1*, *Stat4*, and *Htr1d*, which are involved in signal transduction and neurotransmission. Importantly, all of these genes exhibited substantial regulation in both RNA-seq and qRT–PCR analyses.

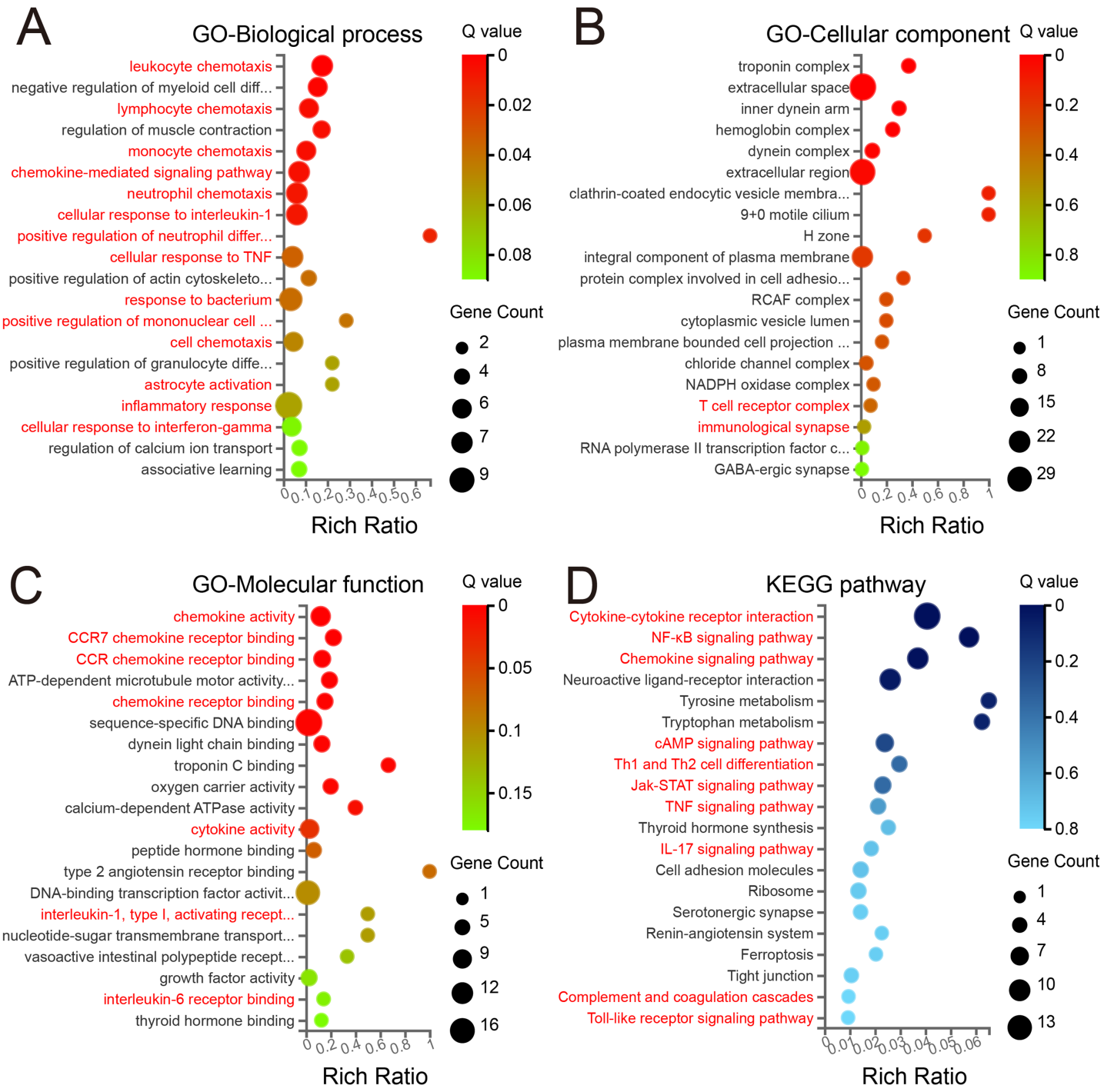

Figure 3 GO and KEGG enrichment analyses of DEGs. The 20 top enriched GO terms are shown in the biological process (A), cellular component (B), and molecular function (C). (D) The 20 top KEGG pathway enrichments with DEGs. Red text denotes terms related to immunological processes. The ordinate represents the Q value, while the abscissa shows the enrichment ratio. Dot size represents the count of genes, and color indicates the Q value. A Q value ≤ 0.05 was considered significantly enriched. Full-size DOI: 10.7717/peerj.18664/fig-3

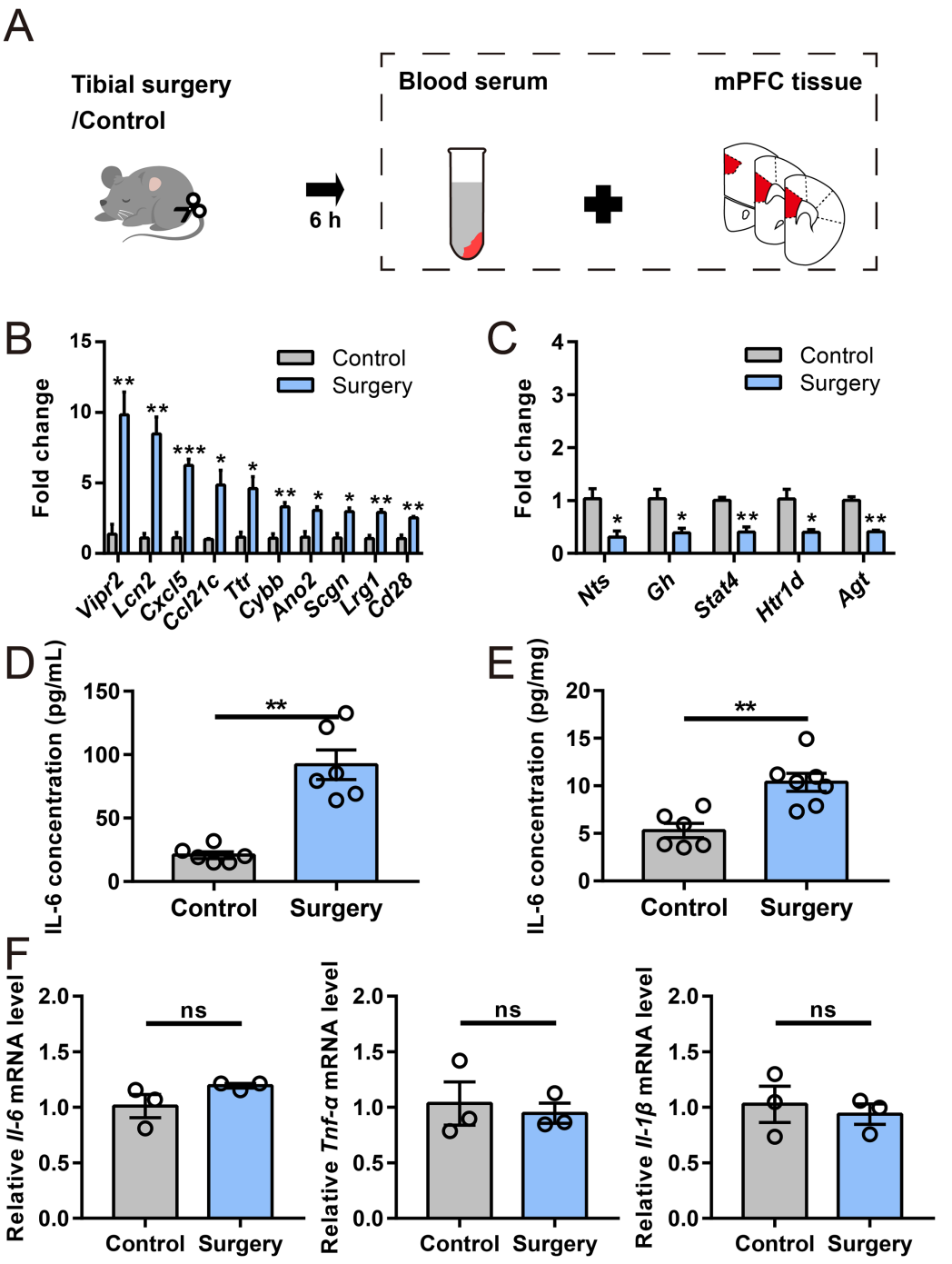

Figure 4 Verification of DEGs and inflammatory cytokine levels. (A) Cartoon depicting samples collection in another cohort at 6 h after surgery. (B and C) qRT–PCR validation of selected DEGs identified by RNA-seq analysis (n = 3 mice/group). (D and E) ELISA for IL-6 in serum and the mPFC, respectively (n = 6–7 mice/group). (F) Relative expression of *Il-6*, *Tnf*-α, and *Il-1β* in the mPFC (n = 3 mice/group). Data are represented as mean ± SEM, ***P < 0.001; **P < 0.01; *P < 0.05; ns, not significant.

Full-size DOI: 10.7717/peerj.18664/fig-4

Levels of inflammatory cytokines

To verify the immune response mediators, levels of representative proinflammatory cytokine were evaluated by ELISA and qRT–PCR (Fig. 4A). Notably, ELISA indicated that IL-6 level was significantly elevated in serum and mPFC 6 h post-surgery (Figs. 4D and 4E). However, no significant alternations were noticed in the mRNA levels of *Il-6*, *Tnf*-α and *Il-1β* in the mPFC after surgery (Fig. 4F). These results suggested that a distinct neuroinflammatory response was induced during early phase of PND.

DISCUSSION

In this study, we demonstrated that cognitive function was impaired after tibial surgery in mice. Since the function of the mPFC region is dysregulated early after surgery (*Sun et al., 2023*), mPFC tissues were isolated 6 h post-surgery for RNA-seq analysis. Significant enrichment of the identified DEGs in immune-related processes and pathways was noticed. Additionally, we observed an increase in IL-6 level in the mPFC, whereas its mRNA level remained unchanged, indicating that a distinct neuroinflammatory response occurred in the mPFC.

Several DEGs have been implicated in various neurological diseases, and the majority were identified for the first time in PND. For example, *Cxcl5*, a prominently upregulated gene, is markedly elevated in response to brain injury and participates in neuroinflammatory responses and cognitive decline (*Wang et al., 2016*; *Cao et al., 2023*). Another upregulated gene, *Ccl21*, facilitates the recruitment of peripheral Th17 cells into the brain parenchyma, thereby exacerbating neuroinflammation and impairing cognitive abilities (*Wang et al., 2022*). Interestingly, elevated lipocalin-2 levels were observed in the mPFC, which contributes to neuroinflammation and cognitive decline in the hippocampus (*Xiang et al., 2022*). However, whether a similar mechanism exists remains unclear. Additionally, *Nts*, a down-regulated DEG, exerts neuroprotective effects in Alzheimer's disease (*Xiao et al., 2014*).

Neuroinflammation is triggered after peripheral surgery, and is involved in developing PND. The mPFC is particularly susceptible to the effects of inflammation, and acute neuroinflammation can disrupt neural network and synaptic activity, resulting in significant cognitive deficits (*Ji et al., 2020*). In GO and KEGG pathway enrichment analyses, we observed significant enrichment in immune-related terms and pathways. First, DEGs were notably enriched in chemotaxis processes, including lymphocyte, monocyte, and neutrophil chemotaxis. Meanwhile, DEGs were enriched in the chemokine and chemokine receptor signaling pathways. Chemokine axes, such as CXCL5/CCR2 and CCL21/CCR7, can drive circulating leukocyte trafficking into the brain (*Wang et al., 2016*, *2022*; *Cao et al., 2023*). Trafficking of immune cells, such as circulating CD8 T-cells and monocyte, into the brain impairs cognitive functions following surgery (*Degos et al., 2013*; *Li et al., 2023*). Second, DEGs were enriched in the Toll-like receptor signaling pathway, cellular response to IL-1, and TNFα signaling pathway. Toll-like receptors can sense danger and foreign molecules, thereby leading to the production of proinflammatory cytokines and impaired learning and memory functions (*Lin et al., 2021*; *Squillace & Salvemini, 2022*). Elevated levels of IL-1β induce an imbalance of excitation–inhibition in

the mPFC (*Mittli et al., 2023*), and blocking IL-1β signaling mitigates neuroinflammatory response and improves the cognitive performance in PND (*Cibelli et al., 2010*; *Barrientos et al., 2012*). Similarly, neutralization of TNFα remarkably ameliorates surgery-induced neuroinflammation and cognitive deficits (*Terrando et al., 2010*, *2011*). Third, IL-17 has emerged as an important player in several neurodegenerative diseases. Elevated levels of IL-17 trigger synaptic and circuitry impairments in early stage Alzheimer's disease and autism (*Choi et al., 2016*; *Brigas et al., 2021*), and neutralization of IL-17 ameliorates sevoflurane-induced neurocognitive impairment (*Zhang et al., 2022*). Fourth, the complement cascade, which is recognized as an important player in synaptic pruning (*Schafer et al., 2012*), is activated after surgery and contributes to PND (*Wu et al., 2023*). Fifthly, although IFN-γ is necessary for social behavior (*Filiano et al., 2016*), elevated levels of IFN-γ prime microglial activation and the production of proinflammatory cytokines, ultimately impairing cognitive functions (*Kann, Almouhanna & Chausse, 2022*). Last but not least, uncontrolled synaptic pruning by astrocytes disrupts inter-neuronal connectivity, resulting in memory impairment (*Lee et al., 2021*). Astrocyte activation following peripheral surgery in the mPFC has been shown to compromise postoperative memory consolidation by promoting the phagocytosis of hippocampal neuronal axon terminals (*Ma et al., 2024*).

Our study has several limitations. First, while IL-6 protein and mRNA levels typically increase in parallel during inflammation (*Gonçalves et al., 2008*), we observed that the mRNA levels of *Il-6*, *Tnf*-α, and *IL-1β* remained unaltered, and IL-6 protein levels were elevated both in serum and mPFC. Neuroinflammation is a complex process, and the observed discrepancy in IL-6 protein and mRNA levels may result from several factors, including the choice of the observation timepoint, post-transcriptional regulatory mechanisms, transport across blood–brain barrier from circulating system, or a combination of these factors. It would be interesting to address these questions in future studies. Additionally, the protein levels of other proinflammatory cytokines including TNF-α and IL-1*β* remain to be determined. Second, considering cellular heterogeneity of the mPFC, single-cell RNA-seq and spatial transcriptomic techniques, such as multiplexed error-robust fluorescence *in situ* hybridization, would help advance our understanding of mPFC dysfunction after surgery and development of PND. Third, other brain regions may also be involved in cognitive decline after surgery. In fact, our previous studies identified 268 DEGs in the hippocampus after surgery (*Xiang et al., 2019*), and revealed that LCN2, one of the top elevated genes in hippocampus, mediates surgery-induced microglia activation and cognitive decline (*Xiang et al., 2022*). However, whether there is a common role of LCN2 in mPFC remains to be determined. Given the well-established roles of mPFC-hippocampal circuits in cognitive function, comparing transcriptomic responses in the mPFC and hippocampus at the circuit level would offer additional insights into PND. Finally, since we identified a series of novel DEGs, further gain- and loss-of-function studies are required to elucidate specific contributions of these genes to PND.

CONCLUSIONS

In summary, we identified a distinct and acute DEG signature in the mPFC after surgery, and revealed distinct features of the functional properties of the mPFC during the early phase of PND. Integrating these findings with further gain- and loss-of-function experiments would greatly help us to better understand of the development and pathogenesis of PND.

ACKNOWLEDGEMENTS

The authors would like to thank Editage for English language editing.

ADDITIONAL INFORMATION AND DECLARATIONS

Funding

The research was supported by the Zhejiang Provincial Natural Science Foundation of China (LQ23H090013 and LBY22H270007). The funders had no role in study design, data collection and analysis, decision to publish, or preparation of the manuscript.

Grant Disclosures

The following grant information was disclosed by the authors:
Zhejiang Provincial Natural Science Foundation of China: LQ23H090013 and LBY22H270007.

Competing Interests

The authors declare that they have no competing interests.

Author Contributions

- Xiaodong Tang conceived and designed the experiments, performed the experiments, analyzed the data, prepared figures and/or tables, authored or reviewed drafts of the article, and approved the final draft.
- Xuwu Xiang performed the experiments, authored or reviewed drafts of the article, and approved the final draft.
- Yang Yu performed the experiments, analyzed the data, prepared figures and/or tables, and approved the final draft.
- Shuyuan Huang performed the experiments, prepared figures and/or tables, and approved the final draft.
- Caifei Pan performed the experiments, analyzed the data, prepared figures and/or tables, and approved the final draft.
- Shuyuan Gan performed the experiments, prepared figures and/or tables, and approved the final draft.
- Yongxing Yao conceived and designed the experiments, authored or reviewed drafts of the article, and approved the final draft.

Animal Ethics

The following information was supplied relating to ethical approvals (*i.e.*, approving body and any reference numbers):

The Animal Care Committee of the First Affiliated Hospital at Zhejiang University School of Medicine (Hangzhou, China) approved this study.

Microarray Data Deposition

The following information was supplied regarding the deposition of microarray data:

The raw sequence files for mRNA sequencing are deposited in the NCBI Sequence Read Archive database: PRJNA1077729.

Data Availability

The following information was supplied regarding data availability:

The raw data are available in the Supplemental Files.

Supplemental Information

Supplemental information for this article can be found online at http://dx.doi.org/10.7717/peerj.18664#supplemental-information.

REFERENCES

Agetsuma M, Sato I, Tanaka YR, Carrillo-Reid L, Kasai A, Noritake A, Arai Y, Yoshitomo M, Inagaki T, Yukawa H, Hashimoto H, Nabekura J, Nagai T. 2023. Activity-dependent organization of prefrontal hub-networks for associative learning and signal transformation. *Nature Communications* **14(1)**:5996 DOI 10.1038/s41467-023-41547-5.

Barrientos RM, Hein AM, Frank MG, Watkins LR, Maier SF. 2012. Intracisternal interleukin-1 receptor antagonist prevents postoperative cognitive decline and neuroinflammatory response in aged rats. *Journal of Neuroscience: The Official Journal of the Society for Neuroscience* **32(42)**:14641–14648 DOI 10.1523/JNEUROSCI.2173-12.2012.

Berian JR, Zhou L, Russell MM, Hornor MA, Cohen ME, Finlayson E, Ko CY, Rosenthal RA, Robinson TN. 2018. Postoperative delirium as a target for surgical quality improvement. *Annals of Surgery* **268(1)**:93–99 DOI 10.1097/SLA.0000000000002436.

Brigas HC, Ribeiro M, Coelho JE, Gomes R, Gomez-Murcia V, Carvalho K, Faivre E, Costa-Pereira S, Darrigues J, de Almeida AA, Buée L, Dunot J, Marie H, Pousinha PA, Blum D, Silva-Santos B, Lopes LV, Ribot JC. 2021. Il-17 triggers the onset of cognitive and synaptic deficits in early stages of Alzheimer's disease. *Cell Reports* **36(9)**:109574 DOI 10.1016/j.celrep.2021.109574.

Cao Q, Chen J, Zhang Z, Shu S, Qian Y, Yang L, Xu L, Zhang Y, Bao X, Xia S, Yang H, Xu Y, Qiu S. 2023. Astrocytic cxcl5 hinders microglial phagocytosis of myelin debris and aggravates white matter injury in chronic cerebral ischemia. *Journal of Neuroinflammation* **20(1)**:105 DOI 10.1186/s12974-023-02780-3.

Chen J, Liu S, Wang X, Huang J, Phillips J, Ma D, Ouyang W, Tong J. 2022. Hdac6 inhibition alleviates anesthesia and surgery-induced less medial prefrontal-dorsal hippocampus connectivity and cognitive impairment in aged rats. *Molecular Neurobiology* **59(10)**:6158–6169 DOI 10.1007/s12035-022-02959-4.

Choi GB, Yim YS, Wong H, Kim S, Kim H, Kim SV, Hoeffer CA, Littman DR, Huh JR. 2016. The maternal interleukin-17a pathway in mice promotes autism-like phenotypes in offspring. *Science* **351(6276)**:933–939 DOI 10.1126/science.aad0314.

Cibelli M, Fidalgo AR, Terrando N, Ma D, Monaco C, Feldmann M, Takata M, Lever IJ, Nanchahal J, Fanselow MS, Maze M. 2010. Role of interleukin-1beta in postoperative cognitive dysfunction. *Annals of Neurology* **68(3)**:360–368 DOI 10.1002/ana.22082.

Courtin J, Bienvenu TC, Einarsson E, Herry C. 2013. Medial prefrontal cortex neuronal circuits in fear behavior. *Neuroscience* **240(423–430)**:219–242 DOI 10.1016/j.neuroscience.2013.03.001.

Degos V, Vacas S, Han Z, van Rooijen N, Gressens P, Su H, Young WL, Maze M. 2013. Depletion of bone marrow-derived macrophages perturbs the innate immune response to surgery and reduces postoperative memory dysfunction. *Anesthesiology* **118(3)**:527–536 DOI 10.1097/ALN.0b013e3182834d94.

Evered L, Silbert B, Knopman DS, Scott DA, DeKosky ST, Rasmussen LS, Oh ES, Crosby G, Berger M, Eckenhoff RG. 2018. Recommendations for the nomenclature of cognitive change associated with anaesthesia and surgery—2018. *British Journal of Anaesthesia* **121(5)**:1005–1012 DOI 10.1016/j.bja.2017.11.087.

Filiano AJ, Xu Y, Tustison NJ, Marsh RL, Baker W, Smirnov I, Overall CC, Gadani SP, Turner SD, Weng Z, Peerzade SN, Chen H, Lee KS, Scott MM, Beenhakker MP, Litvak V, Kipnis J. 2016. Unexpected role of interferon-γ in regulating neuronal connectivity and social behaviour. *Nature* **535(7612)**:425–429 DOI 10.1038/nature18626.

Gonçalves J, Martins T, Ferreira R, Milhazes N, Borges F, Ribeiro CF, Malva JO, Macedo TR, Silva AP. 2008. Methamphetamine-induced early increase of IL-6 and TNF-alpha mRNA expression in the mouse brain. *Annals of the New York Academy of Sciences* **1139(1)**:103–111 DOI 10.1196/annals.1432.043.

Ji MH, Lei L, Gao DP, Tong JH, Wang Y, Yang JJ. 2020. Neural network disturbance in the medial prefrontal cortex might contribute to cognitive impairments induced by neuroinflammation. *Brain, Behavior, and Immunity* **89**:133–144 DOI 10.1016/j.bbi.2020.06.001.

Johansen JP, Cain CK, Ostroff LE, LeDoux JE. 2011. Molecular mechanisms of fear learning and memory. *Cell* **147(3)**:509–524 DOI 10.1016/j.cell.2011.10.009.

Kann O, Almouhanna F, Chausse B. 2022. Interferon γ: a master cytokine in microglia-mediated neural network dysfunction and neurodegeneration. *Trends in Neurosciences* **45(12)**:913–927 DOI 10.1016/j.tins.2022.10.007.

Lee J-H, Kim J-Y, Noh S, Lee H, Lee SY, Mun JY, Park H, Chung W-S. 2021. Astrocytes phagocytose adult hippocampal synapses for circuit homeostasis. *Nature* **590(7847)**:612–617 DOI 10.1038/s41586-020-03060-3.

Li X, Wang H, Zhang Q, Sun X, Zhang M, Wang G. 2023. Inhibition of adult hippocampal neurogenesis induced by postoperative CD8 + T-cell infiltration is associated with cognitive decline later following surgery in adult mice. *Journal of Neuroinflammation* **20(1)**:227 DOI 10.1186/s12974-023-02910-x.

Lin F, Shan W, Zheng Y, Pan L, Zuo Z. 2021. Toll-like receptor 2 activation and up-regulation by high mobility group box-1 contribute to post-operative neuroinflammation and cognitive dysfunction in mice. *Journal of Neurochemistry* **158(2)**:328–341 DOI 10.1111/jnc.15368.

Ma X, Le Y, Hu L, Ouyang W, Li C, Ma D, Tong J. 2024. Astrocytic phagocytosis in the medial prefrontal cortex jeopardises postoperative memory consolidation in mice. *Brain Pathology* **34(6)**:e13253 DOI 10.1111/bpa.13253.

Mittli D, Tukacs V, Ravasz L, Csősz É, Kozma T, Kardos J, Juhász G, Kékesi KA. 2023. LPS-induced acute neuroinflammation, involving interleukin-1 beta signaling, leads to proteomic,

cellular, and network-level changes in the prefrontal cortex of mice. *Brain, Behavior, & Immunity-Health* **28(223)**:100594 DOI 10.1016/j.bbih.2023.100594.

Moller JT, Cluitmans P, Rasmussen LS, Houx P, Rasmussen H, Canet J, Rabbitt P, Jolles J, Larsen K, Hanning CD, Langeron O, Johnson T, Lauven PM, Kristensen PA, Biedler A, van Beem H, Fraidakis O, Silverstein JH, Beneken JE, Gravenstein JS. 1998. Long-term postoperative cognitive dysfunction in the elderly ISPOCD1 study. ISPOCD investigators. International study of post-operative cognitive dysfunction. *Lancet* **351(9106)**:857–861 DOI 10.1016/S0140-6736(97)07382-0.

Paxinos G, Franklin KB. 2019. *Paxinos and Franklin's the mouse brain in stereotaxic coordinates*. Cambridge, MA: Academic Press.

Robinson TN, Raeburn CD, Tran ZV, Angles EM, Brenner LA, Moss M. 2009. Postoperative delirium in the elderly: risk factors and outcomes. *Annals of Surgery* **249(1)**:173–178 DOI 10.1097/SLA.0b013e31818e4776.

Schafer DP, Lehrman EK, Kautzman AG, Koyama R, Mardinly AR, Yamasaki R, Ransohoff RM, Greenberg ME, Barres BA, Stevens B. 2012. Microglia sculpt postnatal neural circuits in an activity and complement-dependent manner. *Neuron* **74(4)**:691–705 DOI 10.1016/j.neuron.2012.03.026.

Silva AR, Regueira P, Albuquerque E, Baldeiras I, Cardoso AL, Santana I, Cerejeira J. 2021. Estimates of geriatric delirium frequency in noncardiac surgeries and its evaluation across the years: a systematic review and meta-analysis. *Journal of the American Medical Directors Association* **22(3)**:613–620 DOI 10.1016/j.jamda.2020.08.017.

Squillace S, Salvemini D. 2022. Toll-like receptor-mediated neuroinflammation: relevance for cognitive dysfunctions. *Trends in Pharmacological Sciences* **43(9)**:726–739 DOI 10.1016/j.tips.2022.05.004.

Sun XY, Liu L, Song YT, Wu T, Zheng T, Hao JR, Cao JL, Gao C. 2023. Two parallel medial prefrontal cortex-amygdala pathways mediate memory deficits via glutamatergic projection in surgery mice. *Cell Reports* **42(7)**:112719 DOI 10.1016/j.celrep.2023.112719.

Terrando N, Eriksson LI, Ryu JK, Yang T, Monaco C, Feldmann M, Jonsson Fagerlund M, Charo IF, Akassoglou K, Maze M. 2011. Resolving postoperative neuroinflammation and cognitive decline. *Annals of Neurology* **70(6)**:986–995 DOI 10.1002/ana.22664.

Terrando N, Monaco C, Ma D, Foxwell BM, Feldmann M, Maze M. 2010. Tumor necrosis factor-alpha triggers a cytokine cascade yielding postoperative cognitive decline. *Proceedings of the National Academy of Sciences of the United States of America* **107(47)**:20518–20522 DOI 10.1073/pnas.1014557107.

Wang LY, Tu YF, Lin YC, Huang CC. 2016. CXCL5 signaling is a shared pathway of neuroinflammation and blood-brain barrier injury contributing to white matter injury in the immature brain. *Journal of Neuroinflammation* **13(1)**:6 DOI 10.1186/s12974-015-0474-6.

Wang W, Liu E, Li X, Chen S, Pang S, Zhang Y. 2022. CCL21 contributes to Th17 cell migration in neuroinflammation in obese mice following lead exposure. *Toxicology Letters* **366**:7–16 DOI 10.1016/j.toxlet.2022.06.003.

Wu X, Gao Y, Shi C, Tong J, Ma D, Shen J, Yang J, Ji M. 2023. Complement C1q drives microglia-dependent synaptic loss and cognitive impairments in a mouse model of lipopolysaccharide-induced neuroinflammation. *Neuropharmacology* **237(20)**:109646 DOI 10.1016/j.neuropharm.2023.109646.

Xiang X, Tang X, Yu Y, Xie S, Liu L, Chen M, Zhang R, Kang X, Zheng Y, Yang G, Gan S, Zhu S. 2022. Role of lipocalin-2 in surgery-induced cognitive decline in mice: a signal from neuron to microglia. *Journal of Neuroinflammation* **19(1)**:92 DOI 10.1186/s12974-022-02455-5.

Xiang X, Yu Y, Tang X, Chen M, Zheng Y, Zhu S. 2019. Transcriptome profile in hippocampus during acute inflammatory response to surgery: toward early stage of PND. *Frontiers in Immunology* **10**:149 DOI 10.3389/fimmu.2019.00149.

Xiao Z, Cilz NI, Kurada L, Hu B, Yang C, Wada E, Combs CK, Porter JE, Lesage F, Lei S. 2014. Activation of neurotensin receptor 1 facilitates neuronal excitability and spatial learning and memory in the entorhinal cortex: beneficial actions in an Alzheimer's disease model. *Journal of Neuroscience: The Official Journal of the Society for Neuroscience* **34(20)**:7027–7042 DOI 10.1523/JNEUROSCI.0408-14.2014.

Xiong C, Zhang Z, Baht GS, Terrando N. 2018. A mouse model of orthopedic surgery to study postoperative cognitive dysfunction and tissue regeneration. *Journal of Visualized Experiments* **132(132)**:56701 DOI 10.3791/56701-v.

Xu H, Zhang Y, Zhang F, Yuan SN, Shao F, Wang W. 2016. Effects of duloxetine treatment on cognitive flexibility and BDNF expression in the mPFC of adult male mice exposed to social stress during adolescence. *Frontiers in Molecular Neuroscience* **9**:95 DOI 10.3389/fnmol.2016.00095.

Zhang Q, Li Y, Yin C, Gao M, Yu J, Guo J, Xian X, Hou Z, Wang Q. 2022. IL-17A deletion reduces sevoflurane-induced neurocognitive impairment in neonatal mice by inhibiting NF-κB signaling pathway. *Bioengineered* **13(6)**:14562–14577 DOI 10.1080/21655979.2022.2090608.